NUMERICAL INVESTIGATION OF ENTROPY GENERATION IN HYDROMAGNETIC DISSIPATIVE MICROPOLAR FLUID FLOW ALONG A NONLINEAR STRETCHING SHEET

E. O. Fatunmbi[1] andS. O. Are[2]
[1]Department of Mathematics and Statistics, Federal Polytechnic, Ilaro, Nigeria.
E-mail: [1]ephesus.fatunmbi@federalpolyilaro.edu.ng, [2]stephen.are@federalpolyilaro.edu.ng
corresponding e-mail: *ephesus.fatunmbi@federalpolyilaro.edu.ng

Abstract
The level of irreversibility that takes place in any thermal process is measured by means of entropy generation. In different industrial and engineering sectors, the phenomena of heating and cooling are very crucial in various energy and electronic devices. In the light of this, the optimization of entropy production with the aim of preventing any energy loss, which can affect the performance of a particular system is very necessary. Hence, this study investigates entropy generation analysis in an electrically conducting and dissipative micropolar fluid over a nonlinear vertically stretching sheet being influenced by thermal radiation, non-uniform heat source/sink, variable magnetic field strength and variable electrical conductivity. The dimensionless equations governing the flow and heat transfer are computationally solved using shooting techniques alongside fourth order Runge-Kutta algorithms embedded in Maple 2016 software. The effects of the main physical parameters on the velocity, temperature, microrotation, entropy generation and Bejan number are graphically displayed and discussed. The facts from the study show that heat transfer irreversibility is stronger than that of viscous dissipation and Joule heating as the radiation parameter rises whereas the opposite is the case with rising values of the micropolar and Brikman parameters.
Keywords: Entropy generation; micropolar fluid; viscous dissipation; nonlinear stretching sheet

1.0Introduction

The study of boundary layer fluid flow induced by stretching sheet has been engaged by researchers and engineers since initiated by Sakiadis (1961) due to the consequential applications in industrial and engineering operations. During fabrication operations in many engineering activities, the movement of heat treated materials as well as those produced by extrusion processes between a feed roll and a wind up on transmit belts characterize that of stretching surface. The applications of such can be found in textile and paper production, extrusion of plastic sheet and metal, drawing of copper wires, glass blowing, drawing of plastic films etc. Based on these usefulness, Crane (1970) reported an analytically solution on a two-dimensional linearly stretching sheet where the velocity and distance from the slit vary proportional to each other. Thereafter, several researchers have investigated this subject checking the impact of different parameters, boundary conditions and geometry (Kumar, 2009; Pal and Mondal, 2014; Fatunmbi and Fenuga, 2017; Makinde, *et al.*, 2018).

Nevertheless, all these have been conducted on a linearly stretching sheet. Meanwhile, it has been reported by Gupta and Gupta (1977) that the sheet may be stretched in a nonlinear manner. In view of such report, researchers such as Vajravelu (2001); Cortell (2007, 2008); Hayat (2008); Laxami and Shankar (2016), etc have examined boundary layer flow and heat transfer in a viscous fluid over a nonlinear stretching sheet with diverse parameter of interest. These researches however have been carried out on Newtonian fluids only without considering the more interesting and useful non-Newtonian fluid.

Investigations have shown that Newtonian fluids are incapable in capturing the characteristics of complex and complicated fluids which are useful for industrial purposes and engineering processes. Such characteristics can only be captured by non-Newtonian fluids. On this ground, the non-Newtonian fluids have become prominent in the recent years due to the huge applications in manufacturing and engineering activities such as in petroleum engineering, food and polymer processing, bio-mechanic engineering, etc (Anuradha and Punithavalli, 2019). Various models of non-Newtonian fluid exist due to flow diversity in nature, the rheological attributes of non-Newtonian fluids cannot be described by a single constitutive relationship between stress and shear rate. These models include: Casson fluids, Jeffery fluids, Williamson fluids, micropolar fluids, etc. Out of these, however, the micropolar fluid is found notable.
Micropolar fluids as pioneered by Eringen (1966, 1972) consist of fluids with microstructure, they contain rigid bar-like, randomly oriented (or spherical) particles suspended in a viscous medium such as polymeric fluids, colloidal fluids, liquid crystals, animal blood where particles deformation is ignored. The possible applications of such fluids in engineering and industrial operations can be found in the bio-mechanic and chemical engineering, extrusion of

polymer, slurry technologies, synovial lubrication, etc (Lukaszewicz, 1999; Reena and Rana, 2009). Motivated by these crucial applications, various researchers have investigated boundary layer flow and heat transfer of micropolar fluid considering various parameters, geometries, wall conditions and assumptions (see Chaudhary and Jha, 2008; Reddy and Chamkha, 2016; Kamran, 2018; Arifuzzaman *et al*., 2018). Meanwhile, all these studies were restricted to analysis of first law of thermodynamics, however, studies that are carried out with the second law of thermodynamics relating to entropy generation are found dependable as compared to those the first law (Kobo and Makinde, 2010).

Entropy production analysis is explained through the second law of thermodynamics, it is a means of quantifying the level of irreversibility that occurs in a thermodynamical system. It is a way of measuring the level of work destruction that is available in a system so as to figure out the entropy generation rate in a system with a bid to upgrade such system. In heat transfer problems, entropy generation is a means of measuring the irreversibility that takes place in a system with the use of the second law of thermodynamics (Kobo and Makinde, 2010). Owing to crucial application of such studies in engineering and manufacturing activities, various scholars (see Bejan, 1982, 1996; Salawu *et al.*, 2019; Salawu and Fatunmbi, 2017; Srinivasacharya and Bindu, 2017; Seth *et al.*, 2018; Makinde and Eegunjobi, 2018; El-Aziz, and Saleem, 2019). have investigated such study on both Newtonian and non-Newtonian fluids. However, none of these researches considered entropy generation in an electrically conducting micropolar fluid over an inclined stretching sheet.

In particular, Afridi *et al.* (2017) numerically addressed entropy generation along an inclined impermeable sheet with MHD Newtonian fluid while ignoring non-Newtonian micropolar fluid inspite of its huge applications. Those researchers also neglected the impact of thermal radiation, Joule heating and heat source/sink effects in their study. These parameters have been found useful in engineering and industrial operations such as in gas turbines, astrophysical flows, power plants, etc. Hence, this study has been carried out to extend the work of Afridi *et al.* (2017) by engaging the non-Newtonian hydromagnetic micropolar fluid with the inclusion of thermal radiation, Joule heating, non-uniform heat source/sink effects and considering a nonlinear surface instead of linear surface reported by those authors.

2.0Mathematical Development of the Model

In this work, the model consists of entropy production analysis on a two-dimensional, steady flow of an incompressible and electrically conducting, dissipative and thermally radiating micropolar fluid moving along a nonlinear stretching sheet ss displayed in Fig. 1. It is assumed that the magnetic field varies with x which is applied transversely to the flow direction and that the electrical conductivity also varies with the velocity component u in the x direction where$x$ is the coordinate along the surface in the flow direction and y is the coordinate normal to it. The sheet stretches with a velocity $u = Qx^p$ along x direction where $Q > 0$ is a constant and p is the nonlinear stretching parameter. Neglecting the induced magnetic field, pressure gradient, electric field and assuming that the flow properties are isotropic and constant and using the Boussinesq and boundary layer approximations together with the stated assumptions, the governing equations are listed in Eqs. (1-4).

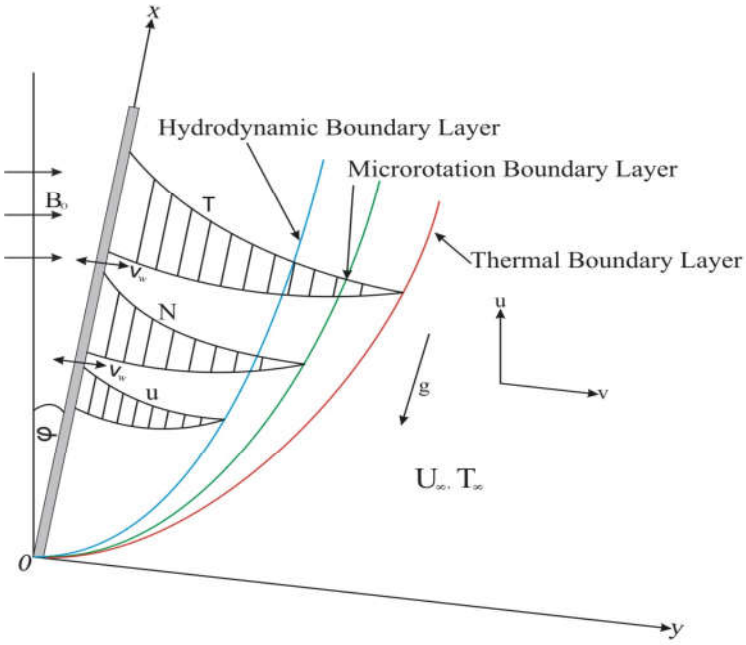

Fig. 1.The Sketch of the Physical Model

$$\frac{\partial u}{\partial x}+\frac{\partial v}{\partial y}=0, \tag{1}$$

$$u\frac{\partial u}{\partial x}+v\frac{\partial u}{\partial y}=\frac{1}{\rho}(\mu+r)\frac{\partial^2 u}{\partial y^2}+\frac{\mathrm{r}}{\rho}\frac{\partial B}{\partial y}+g\beta_T(T-T_\infty)cos\varphi-\frac{\sigma_0{}'(B(x))^2}{\rho}u \tag{2}$$

$$u\frac{\partial H}{\partial x}+v\frac{\partial B}{\partial y}=\frac{\gamma}{\rho j}\frac{\partial^2 H}{\partial y^2}-\frac{r}{\rho j}\left(2B+\frac{\partial u}{\partial y}\right), \tag{3}$$

$$u\frac{\partial T}{\partial x}+v\frac{\partial T}{\partial y}=\frac{k}{\rho c_p}\left(1+\frac{16\sigma^\star T_\infty^3}{3k^\star k}\right)\frac{\partial T^2}{\partial y^2}+\frac{(\mu+r)}{\rho c_p}\left(\frac{\partial u}{\partial y}\right)^2+\frac{\sigma_0{}'(B(x))^2}{\rho c_p}u^2+\frac{q'''}{\rho c_p}, \tag{4}$$

The relevant boundary conditions for this study are as follows:

$$\begin{aligned} &u=u_w=Qx^p, v=v_w,\ B=-\epsilon\frac{\partial u}{\partial y}, T=T_w=\left(Dx^\zeta+T_\infty\right)\ at\ y=0,\\ &u\to 0, B\to 0, T\to T_\infty\ as\ y\to\infty. \end{aligned} \tag{5}$$

From the governing Eqs. (1-4), we note that u and v are velocity components along x and y direction in that order while μ indicates dynamic viscosity, ν describes kinematic viscosity, k denotes thermal conductivity, ρ stands for the density of the ambient fluid whereas the vortex viscosity is written as r while j symbolizes micro-inertial density, c_p connotes the specific heat at constant pressure and γ represents the spin gradient viscosity. Meanwhile, $T, T_w, T_\infty, H, k^\star$ and $\sigma^\star$ describe the fluid temperature, temperature of the stretching sheet, free stream temperature, microrotation component normal to x, y plane, mean absorption coefficient and Stefan-Boltzmann constant in that order.However, in Eq. (5), the wall temperature parameter is indicated by ζ, the suction/injection term is denoted by v_w with $v_w=V_0x^{(p-1)/2}$ (see Yazdi, 2011) where V_0 is a constant while ϵ denotes the micropolar surface parameter.

The electric conductivity is assumed to be (see Das, 2011)

$$\sigma_0{}'=\sigma_0 u, \tag{6}$$

also, the magnetic field is a function of $x$as given by Das (2011) as

$$B(x)=\frac{B_0}{\sqrt{x}} \tag{7}$$

where σ_0 and B_0 are constants.

Following Pal and Mondal (2013), the non-uniform heat source/sink q''' written in Eq. (4) is expressed as

$$q''' = \frac{ku_w}{x^r\nu}[A^\star(T_w - T_\infty)f' + J^\star(T - T_\infty)] \tag{8}$$

with $A^\star = bx^{p-1}$ and $J^\star = b^\star x^{p-1}$ being the space and heat dependent source/sink respectively. With $A^\star > 0, J^\star > 0$ relates to heat source while $A^\star < 0, J^\star < 0$ implies heat sink.

Follow from the work of Hayat (2008), the modelled Eqs. (1-4) have been simplified by means of similarity variables (9).

$$\begin{aligned}
&\eta = y\left[\frac{Q(p+1)x^p}{2x\nu}\right]^{1/2}, B = x^{(3p-1)/2}\left[\frac{Q^3(p+1)}{2\nu}\right]^{1/2} g(\eta),\\
&u = \frac{\partial\psi}{\partial y} = Qx^p f', v = -\frac{\partial\psi}{\partial x} = -\left[\frac{Q\nu(p+1)}{2}\right]^{\frac{1}{2}} x^{\frac{p-1}{2}}\left(f + \frac{(p-1)}{(p+1)}\eta f'\right),\\
&\gamma = \left(\mu + \frac{r}{2}\right)j, \theta(\eta) = \frac{T-T_\infty}{T_w-T_\infty}, j = \left(\frac{\nu}{Q}\right)x^{(1-p)}.
\end{aligned} \tag{9}$$

Eqs. (10-12) are the simplified ordinary differential equations governing the problem.

$$(1+L)f''' + ff'' + Lg' - \left(\frac{2}{p+1}\right)[(p+M)f'^2 - \lambda\theta\cos\varphi] = 0, \tag{10}$$

$$(1+L/2)g'' + fg' - \left(\frac{3p-1}{p+1}\right)f'g - (2g+f'')\left(\frac{2K}{p+1}\right) = 0, \tag{11}$$

$$\begin{aligned}
&(1+R)\theta'' - \left(\frac{2\zeta}{p+1}\right)Prf'\theta + Prf\theta' + (1+L)PrEcf''^2 +\\
&\left(\frac{2}{p+1}\right)PrMEcf'^3 + Pr(\alpha f' + \beta\theta)\left(\frac{2}{p+1}\right) = 0.
\end{aligned} \tag{12}$$

With the boundary conditions becoming

$$\begin{aligned}
&f'(0) = 1, f(0) = Fw, g(0) = -\epsilon f'', \theta(0) = 1,\\
&f'(\infty) = 0, g(\infty) = 0, \theta(\infty) = 0.
\end{aligned} \tag{13}$$

Where

$$\begin{aligned}
&Fw = \frac{-\sqrt{2}V_0}{(\sqrt{Q\nu(p+1)})}, M = \frac{\sigma_0 B_O^2}{\rho}, \lambda = \frac{Gr}{Re^2}, Gr = \frac{g\beta_T(T_w-T_\infty)x^3}{\nu^2}, Re = \frac{u_w x}{\nu},\\
&R = \frac{16T_\infty^3\sigma^\star}{3k^\star k}, L = \frac{r}{\mu}, Ec = \frac{u_w^2}{cp(T_w-T_\infty)}, Pr = \frac{\mu c_p}{k}, \alpha = \frac{bk}{\mu c_p}, \beta = \frac{b^\star k}{\mu c_p}.
\end{aligned} \tag{14}$$

Where the material parameter is indicated by L, the suction/injection parameter is symbolized as fw, λ symbolizes buoyancy parameter, M depicts the Magnetic field parameter while α symbolizes space-dependent source/sink whereas temperature-dependent heat source/sink is designated by β. The thermal Grashof number is indicated by Gr and the Eckert number is represented as Ec whereas the differentiation is done with respect to η and Pr indicates the Prandtl number and R is the radiation parameter.

The important quantities of engineering delight are the skin friction coefficient and the Nusselt number as given in Eq. (15) in that order.

$$C_{fx} = \frac{\tau_w}{\rho u_w^2}, Nu_x = \frac{xq_w}{k(T_w-T_\infty)}, \tag{15}$$

with τ_w being shear stress and q_w heat flux at the surface such that

$$\tau_w = \left[(\mu + r)\frac{\partial u}{\partial y} + rH\right]_{y=0}, q_w = -\left[\left(k + \frac{16T_\infty^3\sigma^\star}{3k^\star}\right)\frac{\partial T}{\partial y}\right]_{y=0}, \tag{16}$$

in view of equations (9) and (16), the skin friction coefficient becomes

$$C_{fx} = \left(\frac{p+1}{2}\right)^{1/2}[1 + (1-\epsilon)L]Re_x^{-1/2}f''(0), \tag{17}$$

whereas the Nusselt number becomes

$$Nu_x = -(1+R)\left(\frac{p+1}{2}\right)^{1/2} Re_x^{1/2}\theta'(0) \tag{18}$$

4.0 Entropy Generation

The entropy generation rate in an electrically conducting, thermally radiating and dissipative micropolar fluid can be described as follows (see Afridi, 2017).

$$S_{gen} = \frac{k}{T^2}\left[(\nabla T)^2 + \frac{16\sigma^\star T_\infty^3}{3k^\star k}(\nabla T)^2\right] + \frac{(\mu+r)}{T}\left(\frac{\partial u}{\partial y}\right)^2 + \frac{\sigma_0\prime(B(x))^2}{T}u^2. \tag{19}$$

On using Eq. (9) in (19) with $p = 1$, it yields

$$Ng = \frac{S_{gen}}{S_{gc}} = \frac{(1+R)\theta\prime^2}{(\theta+\Omega)^2} + \frac{PrEc}{(\theta+\Omega)}(1+L)f''^2 + \frac{2PrEcM}{(\theta+\Omega)}f'^3, \tag{20}$$

where Ng is the overall entropy production in the system, $S_{gc} = kc/\nu$ is the characteristic entropy generation while $\Omega = T_\infty/(T_w - T_\infty)$ indicates dimensionless temperature difference. Bejan number is used to describe the proportion of the entropy production by heat transfer to the total proportion in a system. The first term in Eq. (19 or 20) signifies entropy generation due to heat transfer (N_{ht}) while the second term indicates that of viscous dissipation (N_{vd}) due to fluid friction whereas the last term denotes generation of entropy by Ohmic heating (N_{oh}). This is represented in Eq. (21).

$$Be = \frac{N_{ht}}{Ng} = \frac{N_{ht}}{N_{ht}+N_{vd}+N_{oh}}, \tag{21}$$

where N_{ht}, N_{vd} and N_{oh} depict entropy production due to heat transfer, viscous dissipation and Ohmic heating in that order. Be is the Bejan number in the interval $0 \le Be \le 1$. The dominance of the parameters $N_{vd} + N_{oh}$ over N_{ht} happens when $Be = 0$, the implication of this is that entropy production as a result of heat transfer (N_{ht}) is dominated by those of viscous dissipation and Ohmic heating ($N_{vd} + N_{oh}$). On the other hand, the value of $Be = 1$ implies that generation of entropy due to thermal heat transfer is stronger than that of viscous dissipation and Ohmic heating whereas the value of $Be = 1/2$ points to the fact that $N_{ht} = (N_{vd} + N_{oh})$.

3.0Solution Method and Result Validation

The boundary value Eqs. (10-13) have been solved by shooting technique coupled with Runge-Kutta techniques of fourth order. The solution is achieved by means of computer algebra symbolic Maple 2016 package. To validate the numerical code employed in this research work, the computed values of heat transfer at the sheet surface have been cross-checked with previously reported data of Chen (1998) in the limiting situation as shown in Table 1. There is a good agreement between the results obtained in the present work and the existing work of Chen (1998). Moreso, observation shows that higher values of Prandtl number facilitates heat transfer and similarly, a rise in the positive value of the wall temperature parameter ζ boosts transfer of heat.

Table 1: Computed values of Nu_x compared with Chen (1998) for variation in ζ and Pr when $p = 1, L = Ec = M = \alpha$ and $\beta = fw = 0$

	Chen (1998)			Present		
Pr	$\zeta = -2$	$\zeta = 0$	$\zeta = 2$	$\zeta = -2$	$\zeta = 0$	$\zeta = 2$
0.72	0.72000	0.46315	1.08853	0.71920	0.46325	1.08854
1.0	1.00003	0.58199	1.33334	0.99999	0.58198	1.33333
3.0	3.00046	1.16523	2.50972	2.99999	1.16524	2.50972
7.0	7.00240	1.89537	3.97150	6.99999	1.89540	3.97151
10.0	10.00047	2.30796	4.79686	9.99999	2.30800	4.79687
100.0	100.310	7.76536	15.7118	99.99999	7.76563	15.71195

Table 2: Computed values of C_{fx} as compared with existing results for variation in p when $p = 1, Ec = M = 1.0$, $\varphi = \pi/4$ and $L = 0$

λ	Afridi *et al*. (2017)		Present Study	
	C_{fx}	Nu_x	C_{fx}	Nu_x
0.0	1.4142	0.5546	1.414214	0.555022

0.5	1.2427	0.6976	1.242749	0.697685
1.0	1.0886	0.7931	1.088662	0.793130
1.5	0.9439	0.8974	0.943990	0.867403

Similarly, the values of the skin friction coefficient C_{fx} and Nusselt number Nu_x are also compared with those reported by Afridi *et al.* (2017) for different values of the buoyancy stretching parameter λ. The comparisons demonstrate good relationship as displayed in Table 2. From this table also, it is observed that higher values of the buoyancy parameter tend to lower the C_{fx} whereas the heat transfer is enhanced with a rise in λ.

4.0 Results Analysis and Discussion

The reactions of the main physical parameters on the dimensionless velocity, microrotation, temperature, entropy generation rate and Bejan number are hereby presented in form of graphs with appropriate analysis. In the numerical computations carried out, Use has been made of the following values as the default parameter values: $L = 1.0, M = 1.5, Ec = 0.01, \lambda = 4.0, p = \zeta = R = 0.5, Pr = 0.71, \varphi = \pi/6, fw = 0.2, \alpha = \beta = 0.3$ and $\Omega = 0.5$. Unless otherwise stated on the graphs.

Fig. 2-5 depicts the influence of the material micropolar parameter L on the velocity, microrotation profiles, entropy generation and Bejan number respectively. The plot in Fig. 2 shows that fluid mtion near the inclined sheet drop with rising values of L whereas away from the sheet, the motion of the fluid rises due to reduction in the fluid viscosity. Also observed is the fall in the velocity profiles with higher values of magnetic field parameter M due to the imposition of the Lorentz force. In Fig. 3, the microrotation profile adavnce for the increase in both L and M. The negative values illustrate that there is a reverse rotation of the micro-particles.

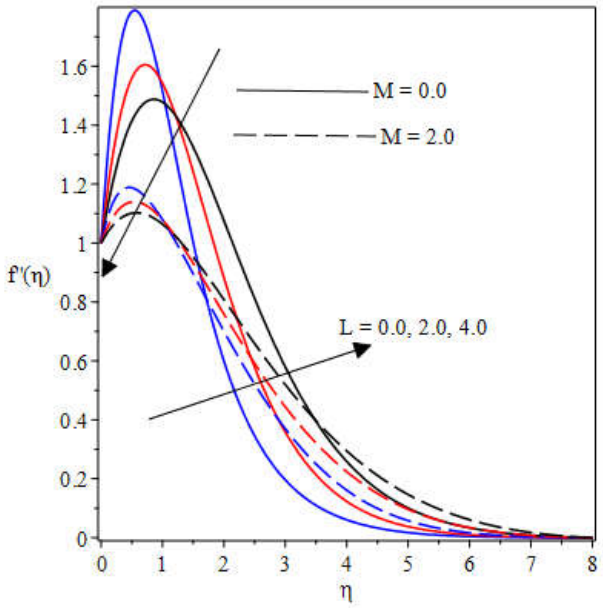

Fig. 2 Influence of L& M on velocity field

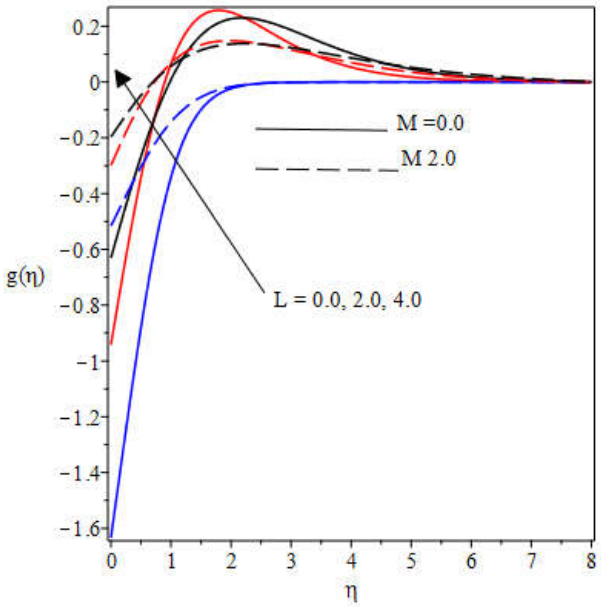

Fig. 3 Microrotation profiles for varying L& M

The plot in Fig. 4 indicates that the entropy generation can be reducd near the stretching sheet with the use of the micropolar fluid. However, there is an increase in the entropy production further away from the sheet. The irreversibilitity due to viscous dissipation and Ohmic heating is stronger than that of heat trasfer irreversibility as L increases. This is so because thre is fall in the Bejan nimber as noted in Fig. 5. Fig. 6 is a plot of the temperature field against η for variation in the radiation parameter R in the presence of the Prandtl number Pr. Clearly, a rise in R boosts the thermal field whereas the temprature reduces with rising values of Pr.

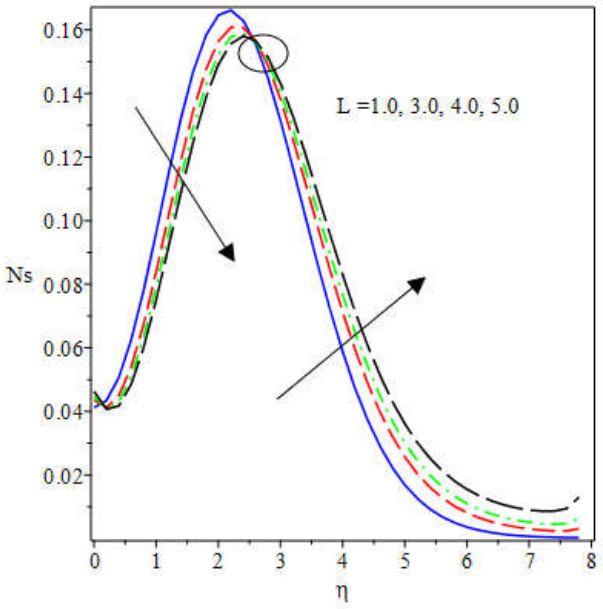

Fig. 4 Impact of L on entropy generation

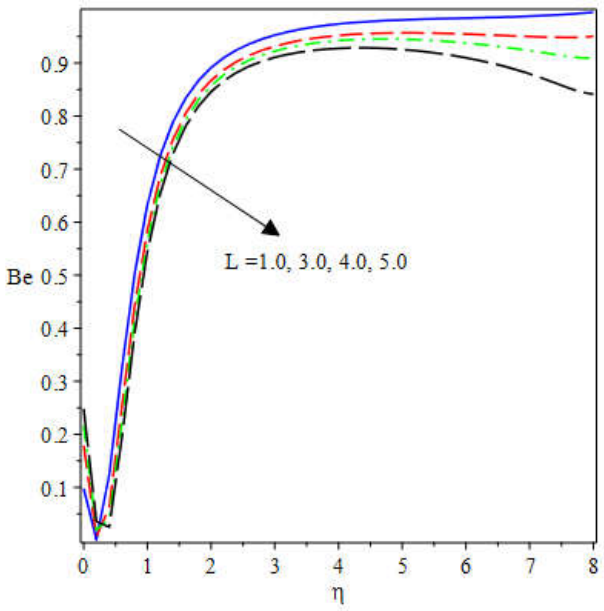

Fig. 5 Effect of L on Bejan number

Basically, a rise in Pr imlies low thermal diffusion, hence, a fall in the thermal boundary layer thickness and in response reduces the temperature. On the other hand, Fig. 7 denmonstrates that the entropy generation rises with rising values of Pr. This occurs since the temperature gradients advances due to a rise in Pr across the boundary layer. Meanwhile, the Bejan number number falls with increasing values of Pr as displayed in Fig. 8.

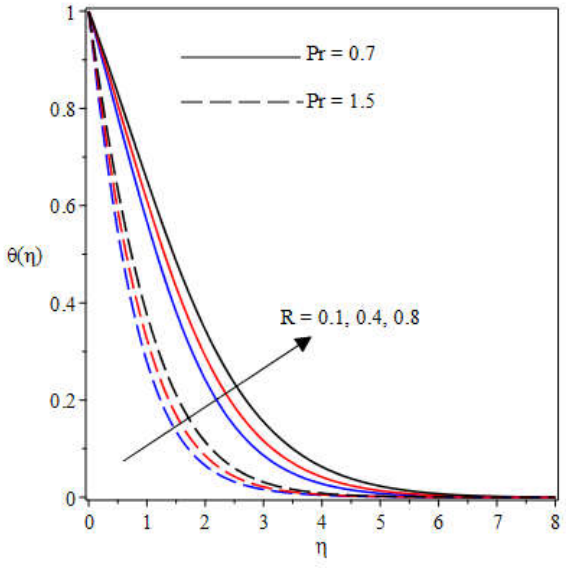

Impact of R & Pr Temprature field

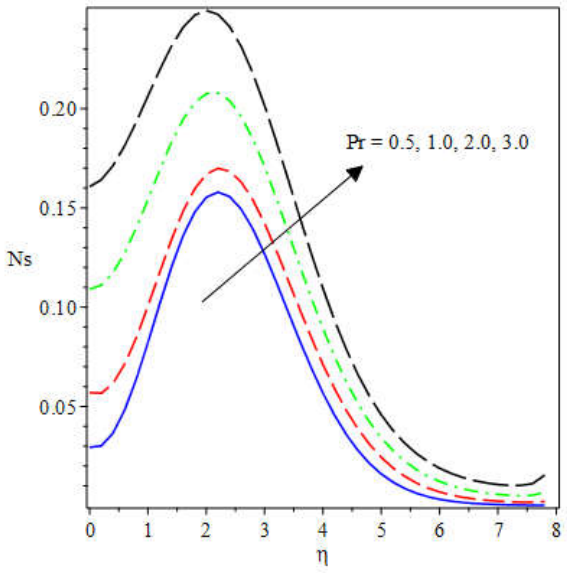

Fig. 7 Effect of Pr on entropy generation

The implication of this is that the magnetic field intensity and the viscous dissipation due to friction in the fluid particles take dominant position in the total production of entropy.. These behaviours tally with the report of Afridi *et al*. (2017).

The plot of the entropy production versus the dimensionless temperature diffrence Ω is described in Fig. 9. Evidnetly, rising values of Ω helps to lower the entropy production thereby prevent loss of energy in the system. At the same time, rising values of Ω ensures that heat transfer irreversiblity is stronger than that of fluid friction and magnetic field

intensity in the total entropy production. This is because there is a reduction in the Bejan number for increasing values of Ω as shown in Fig. 10.

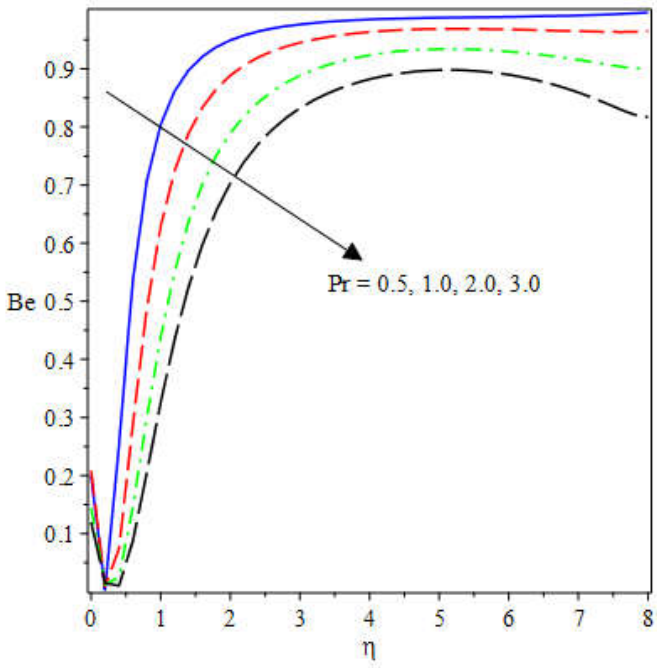

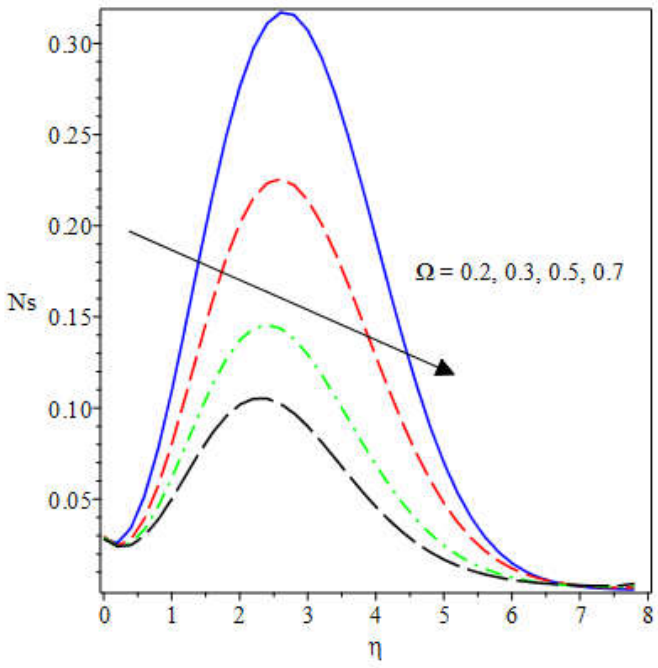

Fig. 8 Variation of Pr on Bejan number **Fig. 9**Effect of Ω on entropy generation

The influence of Eckert number on the entropy production is depicted in Fig. 11. It is shown that with rising values of Ec, the entropy generation rate is increasing. This is so because of there is a friction between the fluid particles which enhances the skin friction coefficient and at such the rate of entropy generation rises. To achieve the aim of the second law therefore, Ekert number should be reduced

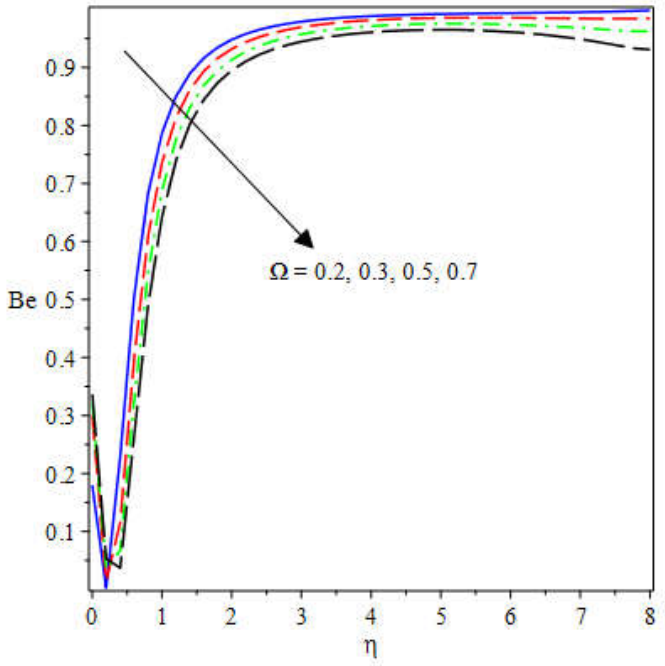

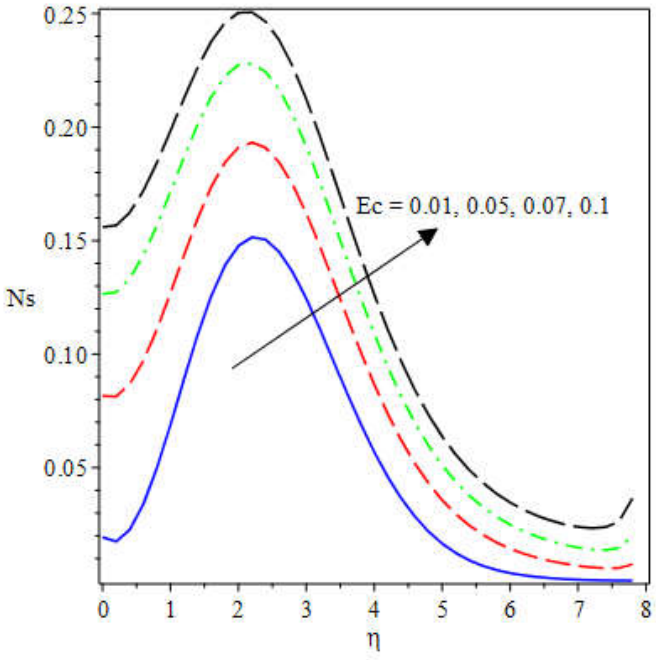

Fig. 10 Impact of Ω on Bejan number

Fig. 11 Effect of Ec on entropy generation

5.0 Conclusion

This study has reported numerically the problem of entropy production in an electrically conducting and dissipative micropolar fluid moving along an inclined permeable sheet which stretches nonlinearly in the flow direction. The governing equations have been translated to ordinary diffrential equations by means of similarity transformations while the resulting equations are solved by the use of shooting techniques in company with Runge-Kutta algorithm. The imapct of main physical parameters have been presented through various graphs while the validation of results obtained showed a good agreement with related exixting work in literature in the limiting conditions. The following points have been deduced from this study:

- The use of micropolar fluid reduces the entropy production especially near the wall of the strtching sheet whereas the rising values of Eckert and Prandtl numbers enhance the production rate of entropy.
- The irreversibility due to fluid friction and magnetic field strength dominate that of heat transfer irreversibility with increase in tha magnitude of micropolar, Prandtl and temperature difference parameters.
- There is fall in the velocity profiles with rising values of magnetic field parameter M due to Lorentz force whereas the temperature field declines for higher values of Prandtl number Pr.
- The rate of heat transferis boosted with growing values of surface temperature parameter ζ while the the skin friction coefficient also develops as the magnitude of the nonlinear stretching parameter p advances.

References

Afridi, M. I., Qasim, M., Khan, H. and Shafie, S. (2017). Entropy generation in magnetohydrodynamic mixed convection flow over an inclined stretching sheet. *Entropy, 19*, 1-11.

Anuradha, S. and Punithavalli, R. (2019). MHD boundary layer flow of a steady micropolar fluid along a stretching sheet with binary chemical reaction. *Int J Appl Eng Res 14*, 440-446.

Arifuzzaman, S. M., Mehedi, F. U. Al-Mamun, A., Biswas, p., Islam, R. and Khan, S. k (2018). Magnetohydrodynamic micropolar fluid in presence of nano particles through porous plate: A numerical study. *Int J Heat Tech, 36*, 936-948.

Bejan, A. (1982). Second law analysis in heat transfer and thermal design, *Adv. Heat Transf., 15*, 1-58.

Bejan, A. (1996). *Entropy Generation Minimization*, CRC: Boca raton, FL, USA.

Chaudhary, R. C. and Jha, A. K. (2008). Effects of chemical reactions on MHD micropolar fluid flow past a vertical

plate in slip-flow regime. *Appl. Math. Engl. Ed., 29*(9): 1179-1194.

Chen, C. H. (1998). Laminar mixed convection adjacent to vertical, continuously stretching sheets. Heat and Mass Transfer 33, 471–476

Cortell, R, (2007). viscous flow and heat transfer over a nonlinearly stretching sheet. *Applied Mathematics and Computation, 184*, 864-873.

Cortell, R. (2008). Effects of viscous dissipation and radiation on the thermal boundary layer over a nonlinearly stretching sheet. *Physics Letters A, 372*, 631-636.

Crane, L. J. (1970). Flow past a stretching plate. *Communicatios Breves, 21*, 645-647.

Das, K. (2011). Slip effects on heat and mass transfer in MHD micropolar fluid flow over an inclined plate with thermal radiation and chemical reaction. *Int. J. Numer. Meth. Fluids, 1-18*. DOI: 10.1002/fld.2683

El-Aziz, M. and Saleem, S. (2019). Numerical Simulation of Entropy Generation for Power-Law Liquid Flow over a Permeable Exponential Stretched Surface with Variable Heat Source and Heat Flux. *Entropy, 21*, 1-19.

Eringen, A. C. (1966). Theory of micropolar fluids. *J. Math. Anal. Appl., 16*, 1-18.

Eringen, A. C. (1972). Theory of thermo-microfluids. *Journal of Mathematical Analysis and Applications, 38*, 480-496.

Fatunmbi, E. O. and Fenuga, O. J. (2017). MHD micropolar fluid flow over a permeable stretching sheet in the presence of variable viscosity and thermal conductivity with Soret and Dufour effects. *International Journal of Mathematical Analysis and Optimization: Theory and Applications, 2017*, 211- 232.

Gupta, P. S. and Gupta, A. S. (1977). Heat and mass transfer on a stretching sheet with suction or blowing. *Can. J. Chem. Eng., 55*, 744-746.

Hayat, T. and Abbas, Z. and Javed, T. (2008). Mixed convection flow of a micropolar fluid over a non-linearly stretching sheet. *Physic Letter A*, 372, 637-647.

Helmy, K. A. (1995). MHD boundary layer equations for power-law fluids with variable electric conductivity. *Meccanica*, 30, 187-200.

Ishak, A. (2010). Similarity solutions for flow and heat transfer over a permeable surface with convective boundary condition,. *Applied Mathematics and Computation, 217*, 837-842.

Kamran, M. (2018). Heat source/sink and Newtonian heating effects on a convective micropolar fluid flow over a stretching/shrinking sheet with slip flow model. *Int J Heat Tech, 36*2, 473-482.

Kobo , N. S. and Makinde, O. D. (2010). Second law analysis for variable viscosity reactive Couette flow under Arrhenius kinetics. *Mathematical Problems in Engineering, 2010*, 1-15.

Kumar, L. (2009). Finite element analysis of combined heat and mass transfer in hydromagnetic micropolar flow along a stretching sheet. *Comput Mater Sci, 46*, 841-848. Doi: 10.1371/journal.pone.0059393

Laxami, T. V. and Shankar, B. (2016). Radiative boundary layer flow and heat transfer of Nanofluid over a nonlinear stretching sheet with slip conditions and suction. *Jordan Journal of Mechanical and Industrial Engineering, 10*, 285-297.

Lu, D., Ramzan, M., Ahmadi, S. Chung, J. D. and Farooq, U. (2018). A numerical treatment of MHD radiative flow of micropolar nanofluid with homogeneous-heterogeneous reactions past a nonlinear stretched surface. *Scientific Reports, 8*, 1-17, Doi:10.1038/41598.018-30965

Lukaszewicz, G. (1999). *Micropolar fluids: Theory and Applications* (1st Ed.). Birkhauser, Boston.

Makinde, O. D and Eegunjobi, A. S. (2018). Entropy Analysis in MHD Flow with Heat Source and Thermal Radiation Past a Stretching Sheet in a Porous Medium. *Defect and Diffusion Forum , 387*, 364-372.

Makinde, O. D., Khan3, Z. H., Ahmad, R and Khan, W. A. (2018). Numerical study of unsteady hydromagnetic radiating fluid flow past a slippery sheet embedded in porous medium, *Physics of Fluids, 30*, 1-7.

Pal, D. and Mondal, H. (2014). Effect of Soret Dufour, chemical reaction and thermal radiation on MHD non-Darcy unsteady mixed convective heat and mass transfer over a stretching sheet. *Commun Nonlinear Sci Numer Simulat, 16*, 1942-1958. doi:10.1016/j.cnsns.2010.08.033

Reddy, P. and Chamkha, A. J. (2016). Soret and Dufour effects on MHD heat and mass transfer flow of a micropolar fluid with thermophoresis particle deposition. *Journal of Naval Architecture and Marine Engineering, 2016*, 1-11.

Reena and Rana, U. S. (2009). Effect of Dust Particles on rotating micropolar fluid heated from below saturating a porous medium. *Applications and Applied Mathematics: An International Journal. 4*, 189-217.

Sakiadis, B. C. (1961). Boundary layer behaviour on continuous solid surfaces: II The boundary layer on a continuous flat surface. *A.I.Ch.E.J. 7*, 221-225.

Salawu, S. O. and Fatunmbi, E. O. (2017). Inherent irreversibility of hydromagnetic Third-grade reactive Poiseuille flow of a variable viscosity in porous media with convective cooling. *Journal of the Serbian Society for Computational Mechanics, 11*(1), 46-58.

Salawu, S. O., Kareem, R. A. and Shonola, S. A. (2019). Radiative thermal criticality and entropy generation of hydromagnetic reactive Powell-Eyring fluid in saturated porous media with variable conductivity. *Energy Reports, 5*, 480-488.

Seth, G. S., Bhattacharyya, A., Kumar, R. and Chamkha, A. J. (2018). Entropy generation in hydromagnetic nanofluid flow over a non-linear stretching sheet with Navier's velocity slip and convective heat transfer,. *Physics of Fluids, 30*, 1-16.

Srinivasacharya, D. and Bindu, K. H. (2017). Entropy generation of micropolar fluid flow in an inclined porous pipe with convective boundary conditions. *Sadhana, 42*(5), 729–740.

Ullah, I., Shafie, S. and Khan, I. (2017). Effects of slip condition and Newtonian heating on MHD flow of Casson fluid over a nonlinearly stretching sheet saturated in a porous medium. *Journal of King Saud University Science*, 29, 250-259.

Vajravelu, K. (2001). Viscous flow over a nonlinearly stretching sheet. *Appl. Math. Comput., 124*,

Yazdi, M. H., Abdulaah, S., Hashim, I. and Sopian, K. (2011). Effects of viscous dissipation on the slip MHD flow and heat transfer past a permeable surface with convective boundary conditions. *Energies*, 4, 2273-2294.